



## THE ROLE OF ADIPOCYTE ENHANCER BINDING PROTEIN 1 (AEBP1) IN CARDIAC FIBROSIS PROGRESSION AND ITS POTENTIAL AS A THERAPEUTIC TARGET

Dallen Calder, Thirupura S. Shankar, Ty Lunde, Christian White, Sutip Navankasattusas, Stavros G. Drakos

Department of Biology

### Introduction

Heart Failure (HF) is a pathophysiological condition generally originating from cardiac stress, such as a heart attack, that leads to an inability of the heart to adequately pump blood throughout the body. In addition to decreased cardiac output, or ejection fraction (EF), HF is also accompanied by structural remodeling, such as fibrosis, cardiomyocyte death, altered cardiomyocyte surface area, thickening/thinning of chamber walls, etc.<sup>1</sup> If left untreated, HF can eventually lead to death. Left Ventricular Assist Devices (LVADs) are used as a HF therapy generally either as a bridge-to-transplant, which ends in a patient receiving a heart transplant, as a bridge-to-cardiac recovery, where patients show improvement and the LVAD is explanted, or as destination therapy, wherein a patient stays on LVAD support and doesn't get transplanted.<sup>2</sup> LVAD therapy relieves the left ventricle (LV) of the task of pumping blood throughout the body, a process called unloading,<sup>3</sup> which allows for cardiac recovery. Patients that exhibit a relative functional and structural improvement (EF >40%, LV end diastolic diameter < 6mm) are designated as responders whereas non-responders are those patients that do not show a marked improvement. Responders make up 15% of the LVAD patients with the remaining 85% being non-responders. This low percentage of recovery necessitates the need for more insights on molecular mechanism driving this process. Unloading of the LV also leads to reverse remodeling which takes place when structural improvements are observed.<sup>4</sup> Fibrosis reversal is one form of reverse remodeling that takes place when a reduction of fibrotic tissue is observed after LVAD unloading. Fibrosis is a compensatory mechanism following an insult of HF that is caused by deposition of extracellular matrix (ECM), however increased fibrosis leads to muscular stiffening and decreasing contractility of the heart, specifically the left ventricle which drives the heart towards failure.<sup>5</sup> During initial cardiac insult, fibroblasts differentiate to myofibroblasts, a change that is marked by differences in phenotypic expression namely increased expression of  $\alpha$ -smooth muscle actin ( $\alpha$ SMA), activation of SMAD pathway (increased pSMAD/SMAD ratio), increased production of ECM proteins such as transgelin (SM22) and collagen.<sup>6,7,8</sup> This differentiation of fibroblasts to myofibroblasts seems to play an integral part in the progression of fibrosis and understanding this process could help inhibit fibrosis progression.

In our human myocardial study, we observed that a small subset of responders with high percent fibrosis at the pre-LVAD timepoint showed a significant decrease in fibrosis at the post-LVAD timepoint suggesting reverse remodeling and improved cardiac function. RNA sequencing of myocardial tissue taken from patients in this high fibrosis group suggested a significant upregulation of Adipocyte enhancer binding protein (*Aebp1*). Also referred to as ACLP, AEBP1

(130kDa) encodes for a secreted protein that acts as a transcription regulator<sup>9,10</sup> as well as mRNA that can also serve as a transcription activator by binding to DNA and cellular receptors.<sup>11</sup>

AEBP1 has previously been studied in fibrosis progression in organs such as the liver and the lungs<sup>12,13,14,15,16</sup> where AEBP1 is reported to promote fibroblast differentiation through activation of TGF $\beta$  and SMAD pathways. In a recent study by Gerhard *et al.*, AEBP1 was identified as the main transcription factor responsible for fibrosis progression in nonalcoholic steatohepatitis.<sup>12</sup> This same study identifies AEBP1 as being upstream of  $\alpha$ SMA. In another study by Tumelty *et al.*, AEBP1 was shown to stimulate the TGF $\beta$  pathway, causing phosphorylation of SMAD proteins, which promote transcription of myofibroblast markers.<sup>17</sup> Wang *et al.* found that myofibroblasts express elevated levels of  $\alpha$ SMA and SM22 and that these cells concomitantly display significant upregulation of AEBP1 (ACLP) and collagen.<sup>18</sup> While these findings suggest AEBP1 plays an important role in fibrosis progression in other organs, additional research is required to elucidate its role in the progression and potential reversal of cardiac fibrosis. Inclusion of the role of AEBP1 in cardiac fibrosis into preexisting literature will assist in the development of fibrosis therapies specifically in terms of multiple organ fibrosis.

Our main hypothesis is that AEBP1 plays an important role in cardiac fibrosis by activating SMAD proteins, leading to increased extracellular matrix production, and that inhibition of AEBP1 decreases transcription of myofibroblast markers by decreasing activation of SMAD proteins. We anticipate our findings will identify AEBP1 as a therapeutic target for inhibiting cardiac fibrosis progression. Using human cardiac fibroblasts (HCF) as an *in vitro* model we observed a significant increase in  $\alpha$ SMA expression in cells stimulated with TGF $\beta$ . Additionally, activated cardiac fibroblasts also showed a significant increase in AEBP1 expression suggesting a connection between activated fibroblasts and AEBP1. We used AEBP1 shRNA knockdown (KD) and AEBP1 viral overexpression (ON) models to monitor the effects of AEBP1 expression in regard to other proteins known to participate in fibroblast differentiation. Our results from AEBP1 ON study indicate that AEBP1 independently activates fibroblasts in the absence of TGF $\beta$ . In contrast, inhibiting AEBP1 resulted in significant reduction in myofibroblast markers in TGF $\beta$  stimulated cells suggesting a unique role of AEBP1 in fibroblast activation. Immunohistochemistry (IHC) was also performed to visualize the presence of AEBP1 in fibrotic tissues from varying time points with results indicating a connection between increased fibrosis and AEBP1. Through AEBP1 ON and KD experiments we show that AEBP1 is an essential component in the molecular processes that underlie fibrosis formation in the heart and can potentially be used to prevent fibrosis progression.

## Methods

**Masson's trichrome/ Fibrosis analysis.** Human myocardial tissue was used for this experiment and formalin fixed for 48h followed by paraffin embedding. 5 $\mu$ m thick sections were cut and stained with Trichrome for fibrosis analysis using the Dako automated special stainer. The slides for fibrosis analysis were scanned under 20x and analyzed using Aperio Image Scope software (version 12.3.2.8013) (using the colocalization v9 algorithm). A ratio of the total stained area to collagen-stained area was reported.

**Human cardiac fibroblast (HCF) culture – stimulation, overexpression (Ad-CMV-hAEBP1-GFP) and knockdown (Ad-CMV-shAEBP1-GFP).** HCF (PromoCell #c-12375) was cultured in HCF media (PromoCell #C-23010) on 12-well plates with 50,000 cells/well for 48h. Cells were stimulated with

10ng/ml TGF $\beta$  at for 48h with media change every 24h. Viral infection (overexpression or knock-down) was performed at 250 MOI for 72h before or after stimulation. The cells were infected with virus for 24h and then the media changed every 24h. Cells were then harvested to perform respective experiments.

**RNA Extraction and qRT PCR.** Human myocardial tissue and HCF were used for this experiment. miRNeasy Mini kit (Qiagen) was used for RNA extraction. The extracted RNA was used for total RNA sequencing (RNA Seq). Agilent RNA ScreenTape Assay was used for QC experiments. Illumina TruSeq Stranded RNA kit was used for library preparation and Ribo-Zero Gold was used to remove rRNA and the sequencing performed on an Illumina HiSeq 2500 with 50bp single-end reads. The same RNA was used for cDNA synthesis (NEB #E3010S) and qRT was performed using *Aebp1* and *Vinculin* primers (**Table 1**).

**Protein Extraction.** HCF were lysed in 1X RIPA buffer (Cell Signaling Technology #9806S) containing 2X protease and phosphatase inhibitor (Thermo Scientific #78440) and was allowed to sit for 20 mins. 5 $\mu$ l of 100 mmol PMSF was added to the homogenate and allowed to rotate for 30 mins at 4°C, followed by 10 mins of centrifugation at 4°C at 18407 rcf. Supernatant was transferred to a new tube and Pierce BCA Protein Assay kit (Thermo Scientific, #23225) was used for protein estimation. Equal volume of 2X Laemmli buffer with 10% DTT was added to the supernatant and boiled for 10 mins at 98°C.

**Western Blotting.** Using 30  $\mu$ g of protein, gels were run at constant volts (25V/gel) and then transferred to a nitrocellulose membrane at constant current (350 mA) for 1h. Membranes were then blocked for 1h using Odyssey Blocking Buffer (LiCor #927-50000) and subsequently probed with primary antibodies overnight. The antibodies used and their concentration are listed in **Table 1**. Blots were then washed with 1X TBS-tween thrice, followed by incubation with secondary antibodies (anti-mouse or anti-rabbit 1:10000) for 30 mins in the dark. An additional three washes with 1X TBS-tween were performed to prepare blots for scanning using Odyssey Infrared Imager. Image Studio Lite software version 5.2 was used to analyze the blots. Lane loading controls were used in each blot and when unavoidable, gels were run simultaneously. The following antibodies were used: AEBP1 (Santa Cruz Bio., sc-271374), VIN (Cell Signaling, 13901s),  $\alpha$ SMA (Abcam, ab5694), HSP60 (Invitrogen, MA3-012), SM22 (Cell Signaling, 62567s), p-SMAD (Cell Signaling, 8828s), SMAD (Cell Signaling, 8685s), FAP (Cell Signaling, 66562s).

**Animals and animal care.** All animal studies were performed in accordance with the University of Iowa Animal Care and Use Committee (IACUC). All procedures involving animals were approved by the Animal Care and Use Committee of the University of Utah and complied with the American Physiological Society's *Guiding Principles in the Care and Use of Animals* and the UK Animals (Scientific Procedures) Act 1986 guidelines. The mice were housed in 12 h dark/light cycle at 70 °F and 40% humidity.

**Mouse myocardial infarction (MI) model.** 12-week-old C57BLJ mice were used for this study. Both male and female mice were used for all experiments. Mice were anesthetized with 3% isoflurane mixed with oxygen, naired and intubated. A thoracotomy was performed and the muscle between the 4th and 5th intercostal muscle was cut to expose the heart. A 6-0 suture was used to ligate the proximal left anterior descending artery (LAD). The muscle and skin were sutured back and the mice allowed to recover in a heating pad.

**Immunohistochemistry (IHC).** Mice/human heart tissue was used for this study. Hearts were paraffinized and sectioned at 5 $\mu$ m thickness. Slides were deparaffinize by serial washing in xylene twice for 5 mins each followed by washing in 95% EtOH twice for 5 mins each. Slides were washed once in 70% EtOH for 5 mins and once in ddH<sub>2</sub>O for 5 mins. Slides were finally washed once in 1X

PBS 5 mins followed by 30mins incubation at 70°C in epitope retrieval solution (IHC-Tek, Cat# IW-1100). The slides were then cooled at RT for 30 mins. After a 5 min PBS wash, a circle section with PAP pen was drawn. 500µl of 5% serum (diluted in 0.2% PBS-Triton) was added to the sections and incubated for 30 mins. Sections were incubated in primary antibodies prepared in 5% serum at a 1:200 dilution, overnight at 4°C. The slides were then placed in a dark room where the rest of the protocol was performed. Slides were washed thrice for 5 mins with 1xPBS and incubated for 1.5h in secondary antibodies in 5% serum at a dilution of 1:200. Slides were then washed twice in 1xPBS and incubated in WGA (1:1000 in 1xPBS) for 1 hr at RT. After a final PBS wash for 10 mins, the slides were cleaned and dried carefully. Mounting medium was placed on the tissue and coverslips were then placed on slides avoiding any bubbles. They were then stored in the dark at 4°C and imaged the following day. All images were taken in the Leica SP8 system using the same settings.

**Immunocytochemistry (ICC).** Cells were cultured on round coverslips for this experiment. Cells were rinsed with 1X PBS twice and fixed in 10% formalin for 20 mins at room temperature (RT). After an additional PBS rinse, 0.5% Triton in PBS was added for 10 mins at RT. After removing the solution, 800 µl of fetal bovine serum (FBS) was added to the plate and cells were blocked for 60 mins at RT. Cells were then incubated overnight at 4C with the primary antibodies in FBS at a concentration of 1:200. The list of antibodies used are listed in **Table 1**. Cells were then washed in 1X PBS thrice for 10 mins each. Cells were incubated in secondary antibodies for 1h at a concentration of 1:200 at RT. Cells were washed twice with 1xPBS and DAPI was added at a concentration of 1:1000 in PBS for 20 mins. After a final PBS rinse, coverslips were mounted onto the slides using mounting medium (Sigma, #F4680). All images were taken in the Leica SP8 system using the same settings.

Western blot				
Protein		Concentration	Company	Catalog#
<b>Adipocyte Enhancer-binding Protein 1</b>	AEBP1	1:100	Santa Cruz	sc-271374
<b>Vinculin</b>	Vin	1:1000	Cell Signaling	13901s
<b>Anti-alpha smooth muscle Actin</b>	α-SMA	1:250	Abcam	ab5694
<b>Heat shock protein 60</b>	Hsp60	1:1000	Invitrogen	MA3-012
<b>Transgelin 2</b>	SM22	1:250	Cell Signaling	62567s
<b>Phospho-Smad2/Smad3</b>	p-SMAD	1:500	Cell Signaling	8828s
<b>Smad2/3</b>	SMAD	1:500	Cell Signaling	8685s
<b>Fibroblast activation protein alpha</b>	FAP	1:500	Cell Signaling	66562s
ICC				
<b>Adipocyte Enhancer-binding Protein 1</b>	AEBP1	1:200	Santa Cruz	sc-271374
<b>Anti-alpha smooth muscle Actin</b>	α-SMA	1:200	Abcam	ab5694
<b>DAPI</b>		1:1000	Invitrogen	D3571

**Table 1:** Table containing name, abbreviation, concentration used, company, and catalogue number of antibodies used in both western blotting and ICC

## Results

Cardiac tissue taken from HF patients was analyzed using Masson's trichrome in order to quantify the fibrosis in each sample. Percent fibrosis was measured in failing hearts both pre- and post-LVAD implantation and was compared against non-failing donor myocardium (Fig 1A). Patients with high pre-LVAD fibrosis (>%25) overall showed a decrease in fibrosis compared to respective post-LVAD samples. A small subset of high fibrosis patients were responders and showed a more significant decrease of fibrosis (Fig 1B-1D). Samples from this high fibrosis responder group were subjected to RNA sequencing along with a control group of donor samples (Fig 1E). AEBP1 was shown to be upregulated in the high fibrosis responder group, suggesting it plays a role in fibrosis during HF. IHC performed on high and low fibrosis samples (Fig 1F) showed more apparent AEBP1 expression in regions of fibrosis compared to normal myocardium. Put together, we observed that AEBP1 corresponds to increased fibrosis.

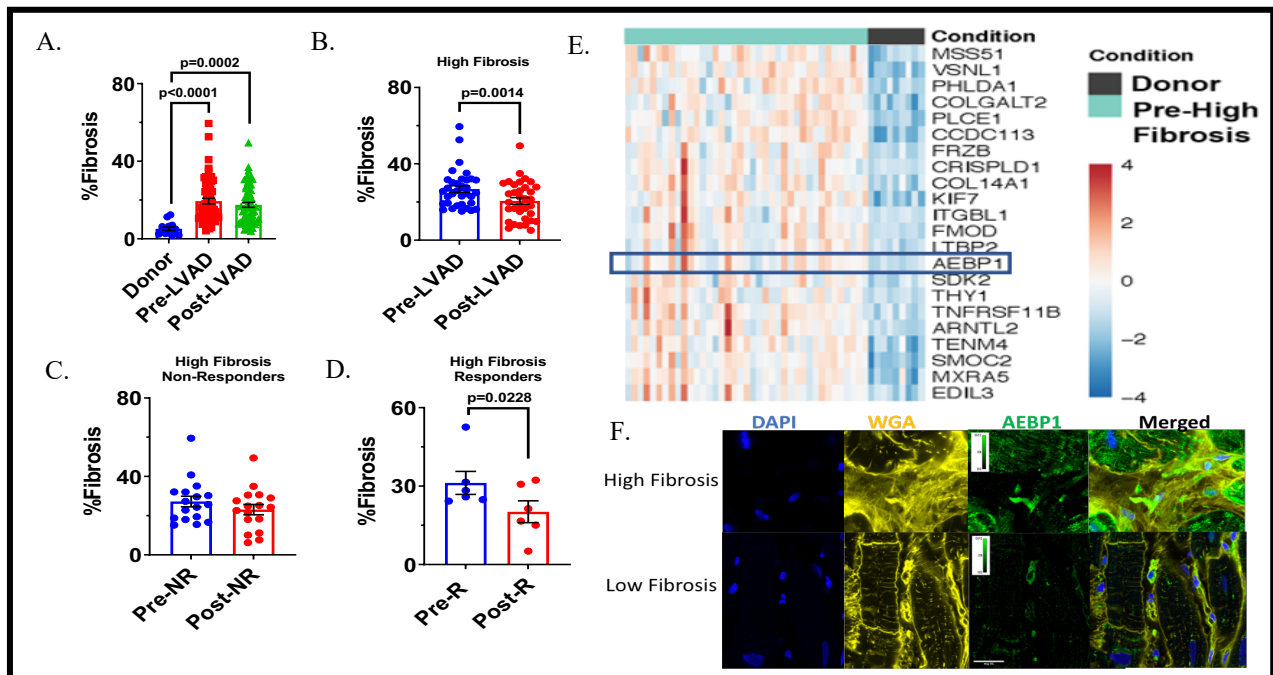


**Figure 1:** A-D Percent Fibrosis in HF patients pre- and post-LVAD, particularly in the high fibrosis group. E Heat map showing upregulation of in HF samples AEBP1. F IHC images demonstrating elevated expression of AEBP1 in high fibrosis group.

Using HCF we showed that TGF $\beta$  stimulation causes protein expression consistent with fibroblast activation, providing a model for cardiac fibrosis. Based on this model we were able to analyze the influence of AEBP1 on fibroblast differentiation and its potential role in reverse remodeling. Western blot analysis of HCF stimulated with TGF $\beta$  showed a significant upregulation of AEBP1 (Fig 2A-2B), indicating AEBP1 is present in differentiated fibroblasts.

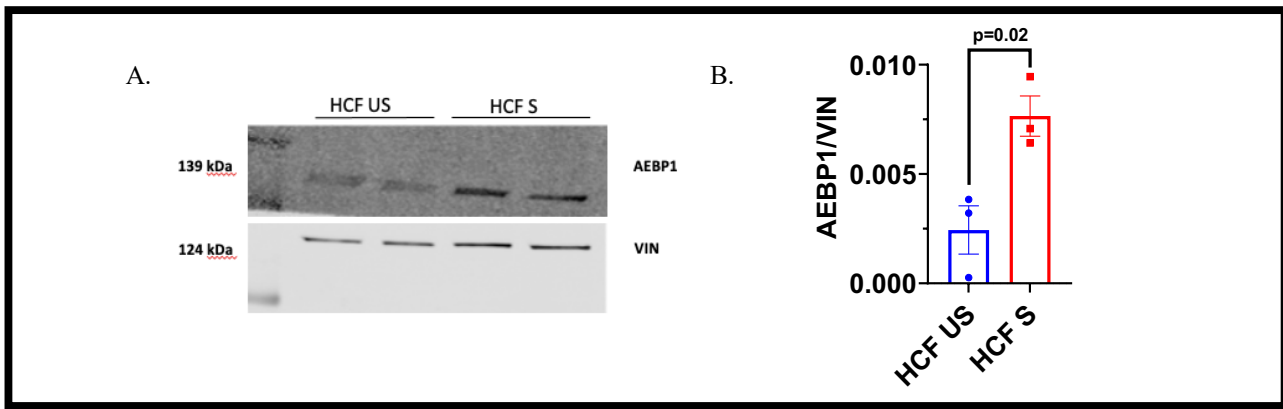


**Figure 2: A-B** Western Blot of AEBP1 in S and US HCF populations.

Using the HCF stimulation model described above, both unstimulated (US) and stimulated (S) samples were stained for DAPI,  $\alpha$ SMA and AEBP1 (Fig 3A-3B). Confocal imaging of cells showed a significant expression of both AEBP1 and  $\alpha$ SMA in the stimulated cells but no expression of either in the unstimulated cells. These results show that in cells expressing AEBP1,  $\alpha$ SMA is also expressed.

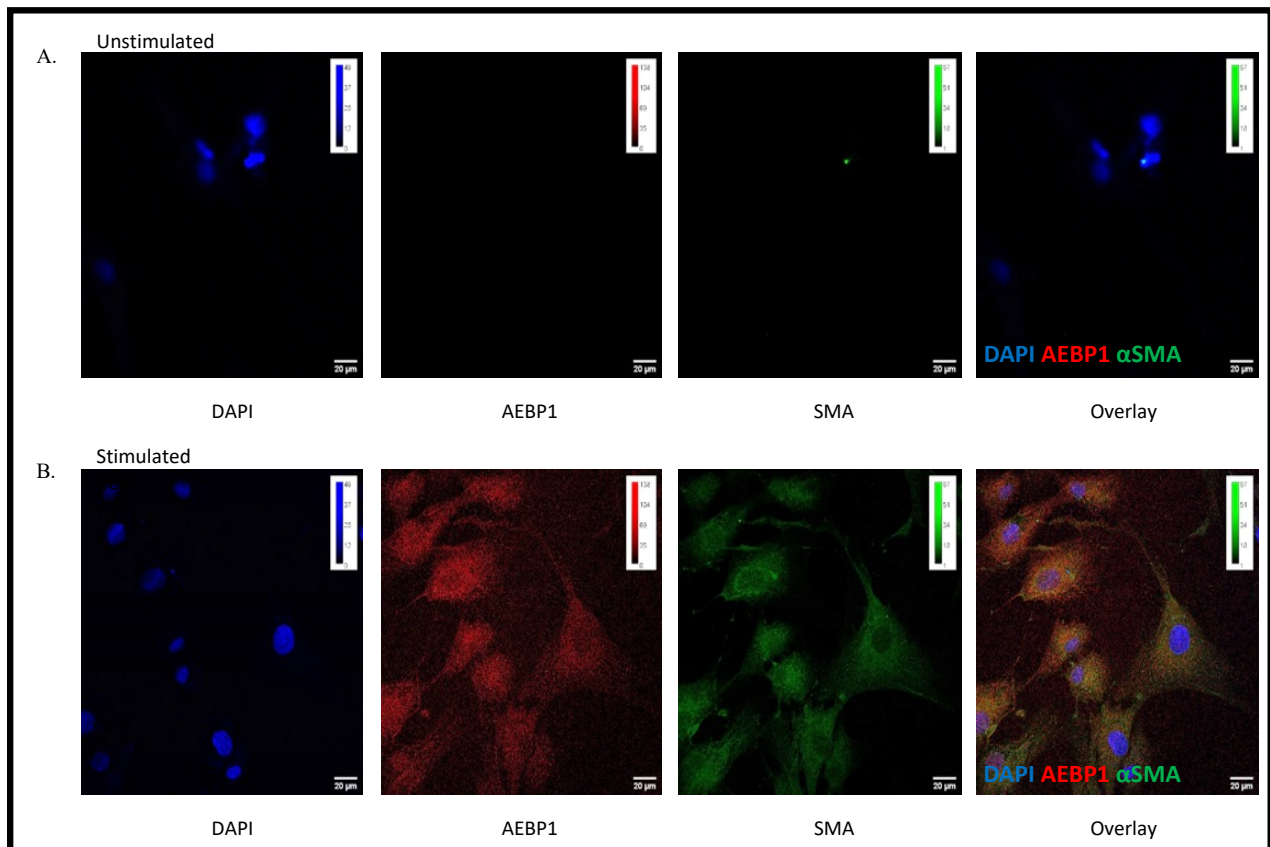


**Figure 3: A-B** ICC images showing the expression of AEBP1 and  $\alpha$ SMA in US and S HCF. DAPI is used as a staining control to ensure that absence of staining with other antibodies is due to a lack of the targeted protein, not improper staining or absence of cells, etc.

Western blotting of stimulated HCF was performed for SM22 and FAP (Fig 4A-4C). As expected, both of these proteins showed significant upregulation in the stimulated samples. Western blot

analysis of collagen showed a significant upregulation in stimulated HCF cells (Fig 4D-4E). Finally, the ratio of phosphorylated SMAD to unphosphorylated SMAD in stimulated HCF cells was determined, showing increased activation of SMAD in stimulated HCF (Fig 4F-4G). Activation, or phosphorylation, of SMAD leads to changes in transcription, ultimately causing an increase in  $\alpha$ SMA expression along with increased production of ECM proteins such as collagen.

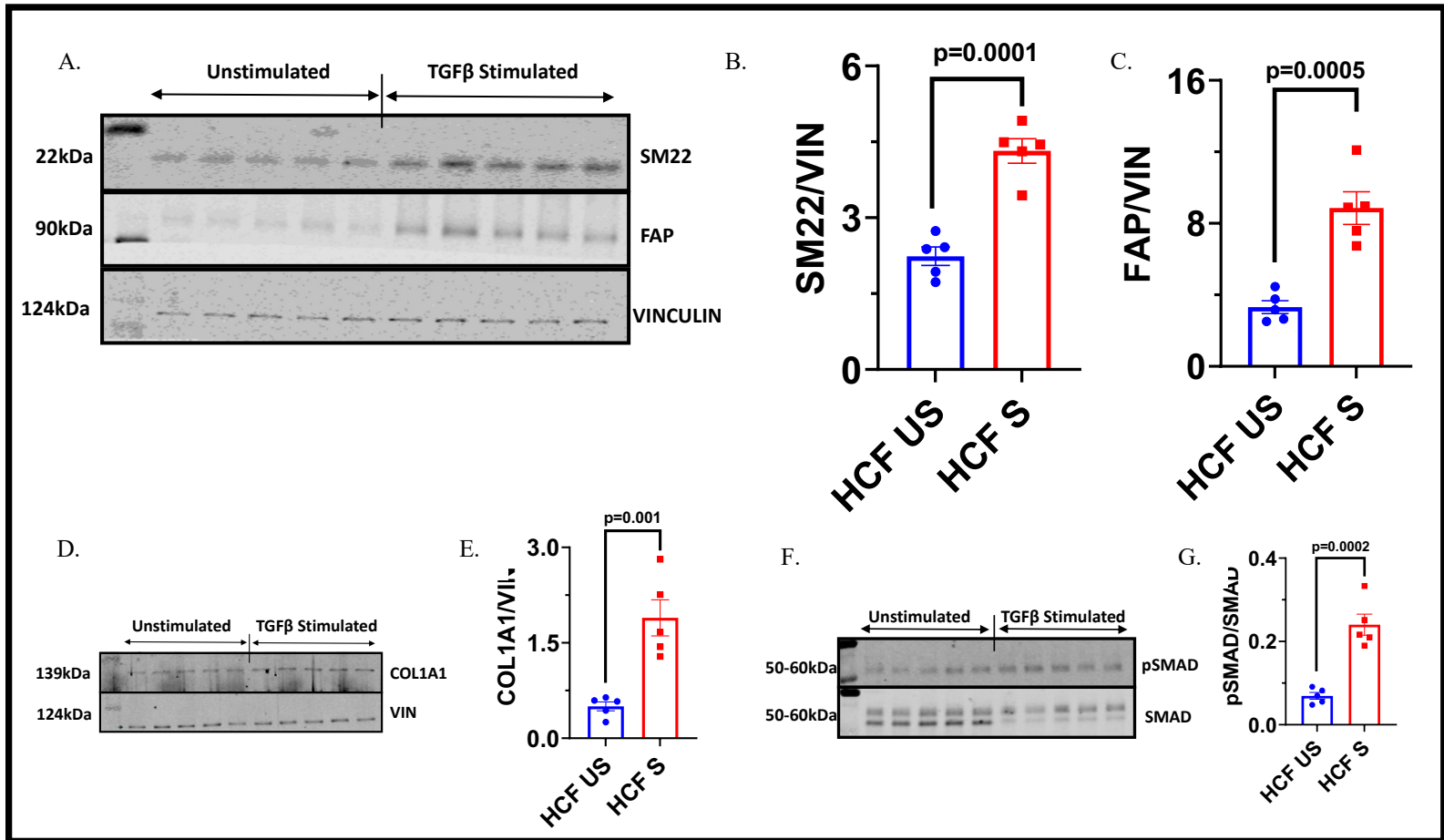


**Figure 4:** A-C Protein levels of SM22, FAP, and VIN were assayed used western blot and further imaged and analyzed to quantify results. D-E Western blot analysis of Col1A1 in stimulated vs. unstimulated HCF. F-G Western blot analysis of pSMAD/SMAD ratios in stimulated vs. unstimulated HCF.

Next, ON and KD models were used to study the effects of AEBP1 on the activation of fibroblasts. In both models GFP virus or shRNA was used as a control for AEBP1 O/N or KD, respectively. In our ON experiments, qRT-PCR data showed a significant increase in AEBP1 mRNA in both groups (US & S) receiving the experimental virus (Fig 5A). Western blot analysis further showed an upregulation of  $\alpha$ SMA in HCF that had received the AEBP1 ON virus (Fig 5B-5C). Interestingly, this upregulation was seen in both the S population and the US population suggesting that AEBP1 can independently induce the myofibroblast phenotype.

Our KD model was created by introducing AEBP1 shRNA into HCF cells thereby inhibiting AEBP1 expression. qRT-PCR showed a significant decrease in AEBP1 expression in both groups (US & S)

receiving the AEBP1 shRNA (Fig 5D). Western blotting was performed for SM22, and our results showed a significant downregulation of in the KD group when compared to the stimulated control group (Fig 5E-5F).

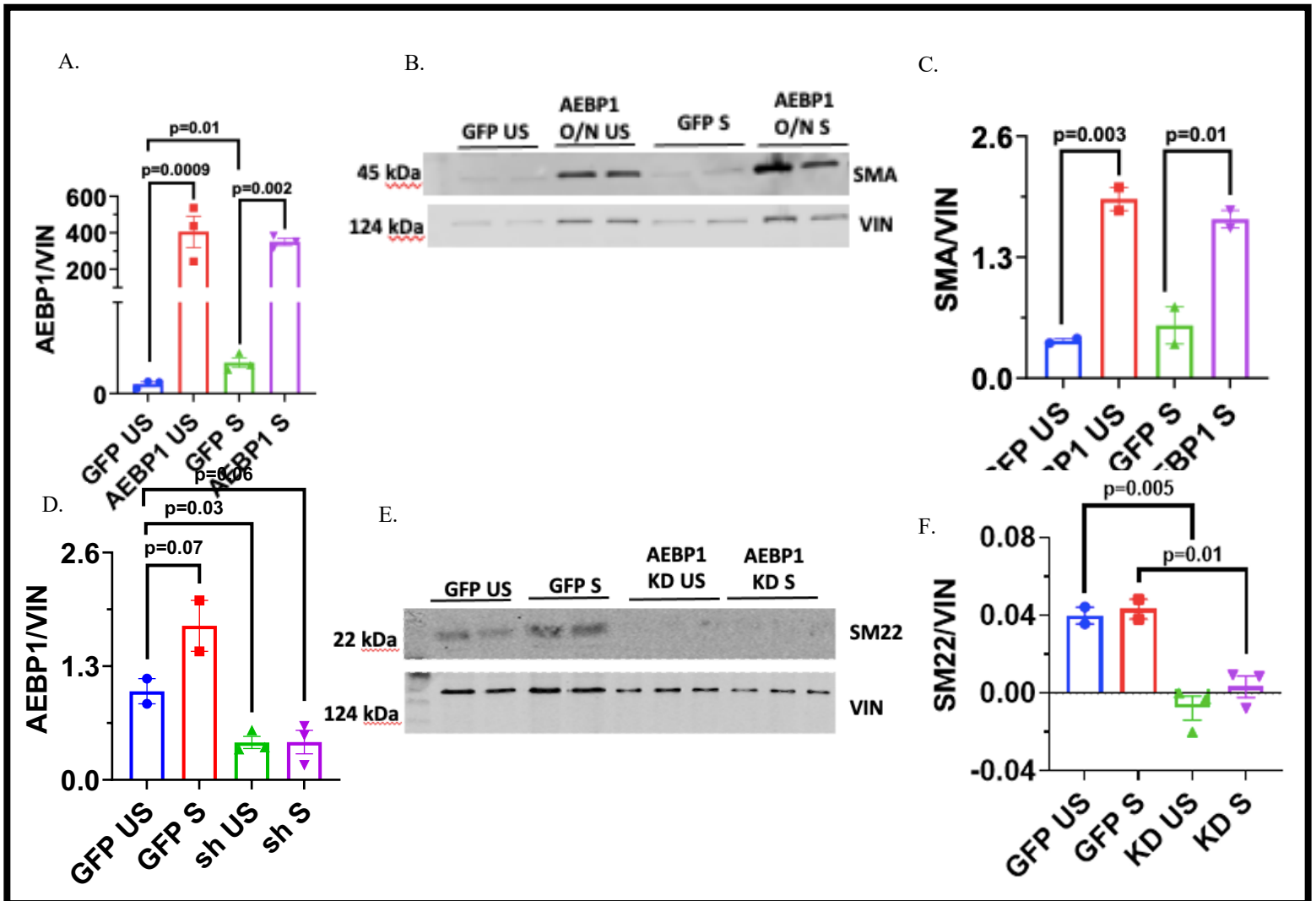


**Figure 5:** **A** qRT-PCR data taken from O/N HCF samples. **B-C** Western blot analysis of  $\alpha$ SMA expression in different HCF populations receiving O/N virus **D** qRT-PCR data taken from KD HCF samples. **E-F** Western blot analysis of SM22 expression in different HCF population receiving KD shRNA.



## Discussion

Heart failure can result from structural changes that arise due to cardiac injury. This cardiac structural remodeling leads to decreased cardiac function. Fibrosis is one of the changes that contributes to cardiac structural remodeling and each HF patient displays distinct levels of fibrosis. In this study we focused on LVAD patients who initially displayed high myocardial fibrosis. Patients with high fibrosis that responded to LVAD therapy showed a significant reduction in myocardial fibrosis upon LVAD unloading. This reverse remodeling is important as it enables the heart to return to, or at least resemble, previous levels of functionality. Understanding the molecular mechanism that governs the process of fibrosis progression may lead to an ability to inhibit fibrosis progression and potentially induce fibrosis reversal. In the liver, it has been proposed that AEBP1 initiates a pathway wherein TGF $\beta$  receptors are activated, subsequently leading to SMAD3 stimulation, increased  $\alpha$ SMA expression, and collagen production.<sup>12</sup> Using IHC, we observed that AEBP1 was upregulated in areas of high fibrosis within HF samples compared to low fibrosis samples. In addition, experiments involving HCF resulted in elevated levels of AEBP1 upon TGF $\beta$  stimulation, suggesting AEBP1 plays a role in activation of fibroblasts. ICC results on HCF showed that  $\alpha$ SMA expression is linked to AEBP1 expression, both of which were expressed in the stimulated population. Western blotting was used to further analyze other proteins known to participate in myofibroblast formation and fibrosis progression. Increased expression of SM22, FAP,  $\alpha$ SMA, Col1A1, and increased phosphorylation of SMAD are all markers of myofibroblast formation and were all characteristic of TGF $\beta$  stimulated HCF. Utilizing an AEBP1 ON model we were able to further elucidate the importance of AEBP1 in fibrosis progression. qRT-PCR data was used to confirm overexpression of AEBP1 mRNA in targeted populations. Additional western blot experiments showed both populations (US & S) that received the AEBP1 ON virus exhibited significant increase in  $\alpha$ SMA expression regardless of TGF $\beta$  stimulation. These results suggest that the presence of AEBP1 is enough to activate fibroblast and initiate fibrosis formation. In our AEBP1 KD experiments we showed that the presence of AEBP1 is not only sufficient to activate fibroblasts, but it is necessary. Knocking down AEBP1 resulted in decreased expression of SM22. While downregulation of SM22 is to be expected in the unstimulated population, here it is also displayed in the stimulated population. This suggests that even in the presence of TGF $\beta$  stimulation, fibroblasts are not activated without AEBP1.

A number of genes are activated during the progression of cardiac fibrosis. However, we show that AEBP1 not only participates but is essential for the transformation of fibroblasts to myofibroblasts and the formation of fibrosis. Our KD results suggest a crucial role of AEBP1 in preventing fibroblast activation and thus as a potential therapeutic target to aid in reverse remodeling in the heart. Understanding AEBP1's role in cardiac fibrosis progression may also lend itself to developing a multi-organ fibrosis therapy. While our data are suggestive of AEBP1's potential as a therapeutic target additional *in vivo* data are necessary and will be obtained via a mouse myocardial infarction (MI) model. An AEBP1 KD virus with a periostin promoter will be injected into mice after an initial period of fibrosis development (2 days or 4 days post MI). Mice will be serially echoed after injection and analyzed for changes in cardiac function and reversal of fibrosis. While additional experiments are necessary to confirm the potential of AEBP1 as a target for fibrosis reversal our current data suggest that AEBP1 is an essential component in the molecular processes that underlie fibrosis formation in the heart and is a potential therapeutic target for reverse remodeling.

## References

---

- <sup>1</sup> Pazos-López, P., Peteiro-Vázquez, J., Carcía-Campos, A., García-Bueno, L., de Torres, J. P. A., & Castro-Beiras, A. (2011). The causes, consequences, and treatment of left or right heart failure. *Vascular health and risk management*, 7, 237.
- <sup>2</sup> Long, J. W., Healy, A. H., Rasmusson, B. Y., Cowley, C. G., Nelson, K. E., Kfoury, A. G., ... & Renlund, D. G. (2008). Improving outcomes with long-term “destination” therapy using left ventricular assist devices. *The Journal of thoracic and cardiovascular surgery*, 135(6), 1353-1361.
- <sup>3</sup> Jhun, C. S., Reibson, J. D., & Cysyk, J. P. (2011). Effective ventricular unloading by left ventricular assist device varies with stage of heart failure: cardiac simulator study. *Asaio Journal*, 57(5), 407-413.
- <sup>4</sup> Koitabashi, N., & Kass, D. A. (2012). Reverse remodeling in heart failure—mechanisms and therapeutic opportunities. *Nature Reviews Cardiology*, 9(3), 147-157.
- <sup>5</sup> Segura, A. M., Frazier, O. H., & Buja, L. M. (2014). Fibrosis and heart failure. *Heart failure reviews*, 19(2), 173-185.
- <sup>6</sup> Nagpal V, Rai R, Place AT, Murphy SB, Verma SK, Ghosh AK, Vaughan DE. MiR-125b Is Critical for Fibroblast-to-Myofibroblast Transition and Cardiac Fibrosis. *Circulation*. 2016 Jan 19;133(3):291-301. doi: 10.1161/CIRCULATIONAHA.115.018174. Epub 2015 Nov 19. PMID: 26585673; PMCID: PMC5446084.
- <sup>7</sup> Santiago, J.-J., Dangerfield, A.L., Rattan, S.G., Bathe, K.L., Cunnington, R.H., Raizman, J.E., Bedosky, K.M., Freed, D.H., Kardami, E. and Dixon, I.M. (2010), Cardiac fibroblast to myofibroblast differentiation in vivo and in vitro: Expression of focal adhesion components in neonatal and adult rat ventricular myofibroblasts. *Dev. Dyn.*, 239: 1573-1584. <https://doi.org/10.1002/dvdy.22280>
- <sup>8</sup> Phan, S. H. (2008). Biology of fibroblasts and myofibroblasts. *Proceedings of the American Thoracic Society*, 5(3), 334-337.
- <sup>9</sup> Kim, S. W., Muise, A. M., Lyons, P. J., & Ro, H. S. (2001). Regulation of adipogenesis by a transcriptional repressor that modulates MAPK activation. *Journal of Biological Chemistry*, 276(13), 10199-10206.
- <sup>10</sup> Cheng, L., Shao, X., Wang, Q., Jiang, X., Dai, Y., & Chen, S. (2020). Adipocyte enhancer binding protein 1 (AEBP1) knockdown suppresses human glioma cell proliferation, invasion and induces early apoptosis. *Pathology, research and practice*, 216(2), 152790. <https://doi.org/10.1016/j.prp.2019.152790>
- <sup>11</sup> Ladha, J., Sinha, S., Bhat, V., Donakonda, S., & Rao, S. M. (2012). Identification of genomic targets of transcription factor AEBP1 and its role in survival of glioma cells. *Molecular Cancer Research*, 10(8), 1039-1051.
- <sup>12</sup> Gerhard GS, Hanson A, Wilhelmsen D, Piras IS, Still CD, et al. (2019) AEBP1 expression increases with severity of fibrosis in NASH and is regulated by glucose, palmitate, and miR-372-3p. *PLOS ONE* 14(7): e0219764. <https://doi.org/10.1371/journal.pone.0219764>
- <sup>13</sup> Teratani, T. et al. Aortic carboxypeptidase-like protein, a WNT ligand, exacerbates nonalcoholic steatohepatitis. *J. Clin. Investig.* 128, 1581–1596. <https://doi.org/10.1172/jci92863> (2018).
- <sup>14</sup> K.E. gjhj, B.D. Smith, M.A. Nugent, et al. Aortic carboxypeptidase-like protein (ACLPL) enhances lung myofibroblast differentiation through transforming growth factor b receptor-dependent and -independent pathways *J. Biol. Chem.*, 289 (2014), pp. 2526-2536, 10.1074/jbc.M113.502617

---

<sup>15</sup> Lou Y, Chen YD, Sun FR, Shi JP, Song Y, Yang J. Potential Regulators Driving the Transition in Nonalcoholic Fatty Liver Disease: a Stage-Based View. *Cell Physiol Biochem*. 2017;41(1):239-251. doi: 10.1159/000456061. Epub 2017 Jan 30. PMID: 28214827.

<sup>16</sup> S.L. Schissel, S.E. Dunsmore, X. Liu, R.W. Shine, M.A. Perrella, M.D. Layne  
Aortic carboxypeptidase-like protein is expressed in fibrotic human lung and its absence protects against bleomycin-induced lung fibrosis *Am. J. Pathol*, 174 (2009), pp. 818-828 10.2353/ajpath.2009.080856

<sup>17</sup> Tumelty, K. E., Smith, B. D., Nugent, M. A., & Layne, M. D. (2014). Aortic carboxypeptidase-like protein (ACLP) enhances lung myofibroblast differentiation through transforming growth factor  $\beta$  receptor-dependent and-independent pathways. *Journal of Biological Chemistry*, 289(5), 2526-2536.

<sup>18</sup> Wang, D., Rabhi, N., Yet, S. F., Farmer, S. R., & Layne, M. D. (2021). Aortic carboxypeptidase-like protein regulates vascular adventitial progenitor and fibroblast differentiation through myocardin related transcription factor A. *Scientific reports*, 11(1), 1-13.